

Oxide Heterostructures from a Realistic Many-Body Perspective

Frank Lechermann

Abstract Oxide heterostructures are a new class of materials by design, that open the possibility for engineering challenging electronic properties, in particular correlation effects beyond an effective single-particle description. This short review tries to highlight some of the demanding aspects and questions, motivated by the goal to describe the encountered physics from first principles. The state-of-the-art methodology to approach realistic many-body effects in strongly correlated oxides, the combination of density functional theory with dynamical mean-field theory, will be briefly introduced. Discussed examples deal with prominent Mott-band- and band-band-insulating type of oxide heterostructures, where different electronic characteristics may be stabilized within a single architected oxide material.

1 Introduction

Since the early days of quantum solid-state research, transition-metal oxides are known to pose very challenging problems in condensed matter physics and materials chemistry (Mott and Peierls 1937). The delicate balance between localization and itinerancy of electrons stemming from partially-filled d -shells in these systems is at the origin of many intriguing phenomena. Spanned by the basic electronic phases, namely band insulator, Mott insulator and conventional metal, the rich transition-metal-oxide phase space encloses e.g. delicate forms of transport and magnetism (Imada et al 1998). The identification of high-temperature superconductivity (coined high- T_c) in CuO_2 -based systems (Bednorz and Müller 1986), eventually well above the liquid-nitrogen temperature, still marks the hallmark finding in this group of compounds.

A new chapter in the research of such materials systems opened in the early 2000s,

Frank Lechermann

I. Institut für Theoretische Physik, Universität Hamburg, D-20355 Hamburg, Germany e-mail: Frank.Lechermann@physnet.uni-hamburg.de

when systematic studies of oxide heterostructures appeared (e.g. (Ohtomo et al 2002)). Ever since, that topical field belongs to a key focus in condensed matter and materials science (see e.g. Refs. (Zubko et al 2011; Hwang et al 2012; Chakhalian et al 2014) for reviews). Important advancements in experimental preparation techniques allow researchers to design oxide materials beyond known appearance in nature. Materials developments from this area may hence be relevant for future technological applications. However, due to the unique combination of the well-known demanding physics of bulk transition-metal oxides with the modern architecturing possibilities, oxide heterostructures furthermore challenge known paradigms in condensed matter physics. The coexistence and mutual affection of intriguing bulk-like electronic phases, each up to now associated with a given oxide compound, within a single oxide heterostructure may be imagined. Moreover, due to the seminal role of the interface in these novel systems, new exotic phases, unknown in present bulk compounds, may emerge.

As of today, already a faithful theoretical investigation of bulk transition-metal oxides with a weakly screened local Coulomb interaction remains a difficult task. Restriction to (effective) single-particle schemes often misses key oxide phenomenologies, such as e.g. the many-body concept of Hubbard bands or local-moment formation. Therefore, the standard first-principles tool of materials science, density functional theory (DFT) in the Kohn-Sham representation, is in many cases not sufficient. Realistic methods beyond conventional DFT that highlight the importance of strong local Coulomb interactions in connection with true many-body electron states are on their way of becoming rather routinely applicable to the correlated electronic structure of bulk oxides. But the sophisticated structural aspects of oxide heterostructures still promotes the task to another level of complexity.

The goal of this review is to highlight the many-body character of some oxide heterostructure problems and to discuss recent first-principles approaches to deal with the physics. We focus on works based on the combination of DFT with the dynamical mean-field theory (DMFT). This is motivated by the fact that the DFT+DMFT framework has evolved to the state-of-the-art realistic many-body approach to cope with the strong-coupling problem of challenging oxide electron systems. In order to set the stage, the starting section 2 provides a brief reminder on the phenomenology of strongly correlated electrons, and some thoughts on the relevance of heterostructure physics. Section 3 delivers an account of the DFT+DMFT technique, while section 4 presents an selected overview of existing applications to oxide heterostructure problems.

2 Preliminary considerations

In the given context, it is relevant to appreciate the many-body phenomenology of correlated electrons and its difference to sole effective-single particle picturings. Therefore, a quick summary of the key characteristics of strongly correlated electron

systems renders the text more self-contained. Second, some general thoughts on the research motivation in the field of oxide heterostructures seem in order.

2.1 Brief reminder on strong electronic correlations in a solid

In various transition-metal oxides, the key many-body aspects reside within the electronic subsystem. The Pauli principle and the mutual Coulomb interaction among the electrons give rise to an intricate many-particle wave function. While the former exchange physics, in its pure appearance, may be cast into a Slater determinant, the explicit interaction leads to more intriguing modifications of the wave function. Electronic correlations, as defined from quantum chemistry, are routed in the latter. Though the Coulomb interactions is long-ranged, screening processes in the solid restrict in most cases its actual relevant range to rather short distances. To a good approximation for many systems, a sole *local* interaction appears sufficient to describe the dominant physics. Given that viewpoint, the Hubbard model stands out as the seminal picturing of the competition between localization and itinerancy among interacting condensed matter electrons, i.e.

$$H_{\text{Hubbard}} = -t \sum_{\langle i,j \rangle \sigma} \left(\hat{c}_{i\sigma}^\dagger \hat{c}_{j\sigma} + \text{h.c.} \right) + U \sum_i \hat{n}_{i\uparrow} \hat{n}_{i\downarrow} \quad , \quad (1)$$

whereby i, j are site indices, $\sigma = \uparrow, \downarrow$ is the spin projection and $\hat{n}_\sigma = \hat{c}_\sigma^\dagger \hat{c}_\sigma$. The nearest-neighbor hopping t describes the electron tendency to delocalize on the lattice, giving rise to the noninteracting band structure, whereas the Hubbard U marks the local Coulomb interaction. The given basic Hamiltonian is appropriate for an (effective) one-band problem. Description of multi-band systems asks in addition for an implementation of the local Hund's physics, as enforced by the Hund's exchange J_{H} .

Depending on the ratio U/t , Fig. 1 displays the principle behavior of the k -integrated spectral function $\rho(\omega) = \sum_{\mathbf{k}} A(\mathbf{k}, \omega)$ on a three-dimensional lattice for the so-called half-filled case $n = 1$, i.e. nominally one electron per lattice site. For small U/t , the system is a very good metal, close to a Fermi gas, with maximum spectral weight

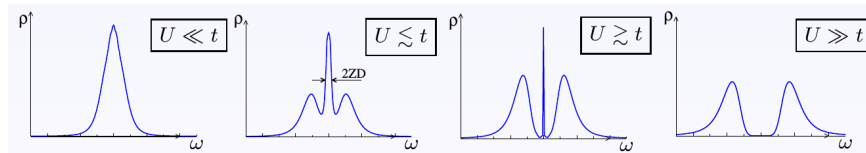


Fig. 1 Local spectral function $\rho(\omega)$ of the Hubbard model on a three-dimensional lattice for different U/t ratios. The quantity D marks the half bandwidth. The nomenclature $A(\omega) = \rho(\omega)$ is often understood, if the explicit k -dependence in the complete spectral function is not discussed.

at the Fermi level ε_F . Note that in that regime, the spectral function reduces to the common density of states (DOS). On the contrary for large U/t , the lattice is in an insulating state, since the electrons localize in real space because of the strong Coulomb repulsion. In spectral terms, removing/adding an electron is associated with states in the lower/upper Hubbard band. Importantly, this *Mott-insulating* state is strikingly different from a conventional band insulator which arises due to complete band filling in reciprocal space.

For U/t inbetween the named limits, the system is in the most interesting regime of a correlated metal. Subtle spectral-weight balancing between the emerging Hubbard bands as well as the coherent quasiparticle (QP) peak close to ε_F takes place. The QP peak is the reminder of the original band states, i.e. encloses states with a well-defined wave vector k , but strongly renormalized and with a weight $Z \leq 1$. The apparent *band-narrowing* included in Z deviating from unity is readily understood: the effective hopping t is reduced due to the electron's hesitation to delocalize when having to pay the Coulomb penalty U while meeting another electron on the nearby lattice site. An existing QP weight Z defines a *Fermi liquid*, since more formally, the quantity Z is derived from the electronic self-energy $\Sigma(\mathbf{k}, \omega)$ via $Z = (1 - \partial\Sigma/\partial\omega|_{\omega \rightarrow 0})^{-1}$ (see e.g. (Imada et al 1998) for more details). Notably, the electronic self energy integrates all many-body effects and is the key quantity of the interacting system. Most common metals are Fermi liquids, but its obvious that there may exist other forms of correlated metals, where a linear self-energy term at low energy is missing. Robust QPs are then absent and the metal is, somewhat vaguely, termed *non-Fermi liquid* (NFL). Various unusual electronic phases of transition-metal oxides are associated or in proximity to NFL characteristics, such as e.g. in the phase diagram of the high- T_c cuprates.

2.2 Why oxide heterostructures?

Deviations from the standard band picture of lattice electrons are often encountered in bulk oxides. Therefore by heterostructuring these materials, an unique playground for investigating, tailoring and designing correlation effects is opened. The challenges are twofold in this respect. First, *known* bulk correlation phenomena are transferred into the heterostructure environment and may be tuned by various means. Second, by interfacing different electronic bulk phases, *new* interface phases are generated, eventually even without a distinct bulk analogon. A very strict separation between these both research directions is albeit delicate.

In the first challenge, common correlation features such as e.g. strong spectral-weight transfer, formation of Hubbard satellites, enhanced susceptibilities, local-moment formation, Kondo physics, magnetic ordering, metal-insulator transition, charge-density-wave or superconducting instabilities are studied within heterostructure architectures. Proximity to an interface, different structural/geometrical relaxations/constraints, symmetry breakings due to layering (cf. Fig. 2) or polarization effects because of a heterostructure-adapted electric field are only a few impacts

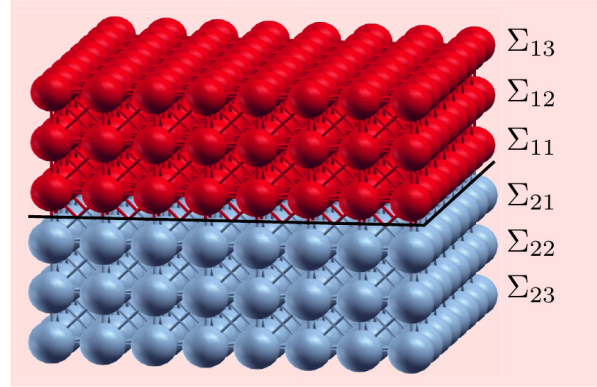


Fig. 2 Principle issue of symmetry breaking induced by an interface in an oxide heterostructure, leading to layer-dependent electronic self-energies Σ_{ij} .

that are able to influence and modify the original bulk electron system. Already a lot of work has been performed in this context and much is cited in the review articles given in the introduction.

For a concrete example, the physics of doped Mott insulators is a key research field in strongly correlated condensed matter. Bulk doping however poses many difficulties in view of a well-defined theoretical description. Most importantly, the intertwining with disorder mechanisms in the electronic and structural sector often hinders a straightforward modelling. Those problems may be overcome in Mott-oxide heterostructures, since electron-, hole-, or structural (i.e. effects only due to the different ion size of the valence-identical dopant) doping can nowadays be realized by respective doping layers, e.g. via molecular-beam epitaxy (cf. (Eckstein and Bozovic 1995; Stemmer and Millis 2013) for reviews). Therewith, the correlated doping physics becomes accessible in a well-defined manner by model-Hamiltonian and/or first-principles techniques. In general, accompanied by this progress, the examination of the influence of defects in strongly correlated materials has gained renewed interest, being explored by considering the detailed defect chemistry together with a state-of-the-art treatment of electronic correlations.

The second challenge is even more demanding and might be associated with the physics of conducting quasi-two-dimensional electron interface systems emerging in oxide heterostructures consisting of bulk band insulators. In principle, selected surface systems may also be counted in this regard. Yet the clarification of the uniqueness of such engineered electron phases beyond respective bulk counterparts is still ongoing research. Topological nontrivial electronic states are surely to be considered, but there the explicit interplay between the topological aspect and electronic correlations is still largely uncharted territory. In the following, these latter material possibilities will not be covered, but the interested reader finds some ideas on this in a recent review (Keimer and Moore 2017).

3 Theoretical approach: realistic many-body theory

3.1 Electronic density functional theory (DFT)

Electronic density functional theory marks an everlasting milestone in condensed matter research, it is and will remain a key step in the first-principles investigation of matter. There are excellent reviews and books on DFT, so there is no need here to iterate thereon. In essence, the framework maps the problem of interacting electrons onto the problem of noninteracting particles within a complicated effective potential. In the present context it is vital to note that although DFT represents *in principle* a complete many-body account of interacting electrons, the most common Kohn-Sham representation based on the conventional local-density or generalized-gradient approximations (i.e. LDA or GGA) mark this method as an effective single-particle approach. In condensed matter, it therefore describes band electrons, whereby the original many-body effects are cast into the named effective potential.

3.2 Dynamical mean-field theory (DMFT)

When it comes to strongly correlated lattice electrons, the dynamical mean-field theory (Metzner and Vollhardt 1989; Georges and Kotliar 1992) has the reputation of being the many-body scheme with the best compromise between generality, accuracy and performance. Also DMFT describes a mapping, and it is here from the problem of interacting lattice electrons onto the problem of a quantum impurity within a self-consistent energy-dependent bath, as sketched for the Hubbard model in Fig. 3.

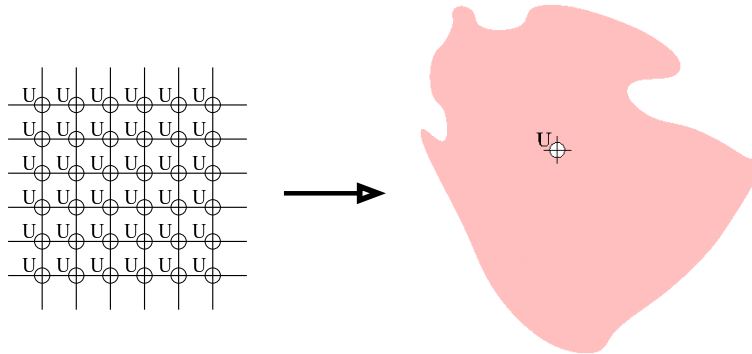


Fig. 3 Sketch of the DMFT mapping of an interacting lattice problem (left) onto a problem of an impurity within an energy-dependent bath (right), assuming a sole onsite Coulomb interaction U .

The one-particle Green's function provides seminal access to the spectral properties and the total energy of an interacting electron system on a lattice. For chemical potential μ , and Hamiltonian $H(\mathbf{k})$ at wave vector \mathbf{k} it reads

$$G(\mathbf{k}, i\omega_n) = [i\omega_n + \mu - H(\mathbf{k}) - \Sigma(\mathbf{k}, i\omega_n)]^{-1} . \quad (2)$$

Note that here and in the following part of the text, fermionic Matsubara frequencies $\omega_n := (2n + 1)\pi T$ are employed to emphasize the treatment at *finite* temperature. The analytical continuation to real frequencies ω in actual calculations may e.g. be performed via the maximum entropy method (see e.g. (Imada et al 1998; Georges et al 1996) for more general details).

In DMFT, the local Green's function is approximated with the help of a k -independent impurity self-energy $\Sigma_{\text{imp}}(i\omega_n)$, i.e.

$$G_{\text{loc}}^{\text{DMFT}}(i\omega_n) = \sum_{\mathbf{k}} [i\omega_n + \mu - H(\mathbf{k}) - \Sigma_{\text{imp}}(i\omega_n)]^{-1} , \quad (3)$$

whereby the corresponding impurity problem reads

$$\Sigma_{\text{imp}}(i\omega_n) = \mathcal{G}_0(i\omega_n)^{-1} - G_{\text{imp}}(i\omega_n)^{-1} . \quad (4)$$

The Weiss field $\mathcal{G}_0(i\omega_n)$ is a unique function of the local Hamiltonian (expressed within a localized basis) and, importantly, the DMFT self-consistency condition implies $G_{\text{imp}} = G_{\text{loc}}^{\text{DMFT}}$. The calculational loop is depicted in the 'DMFT loop' box of Fig. 4 and quantum impurity solvers based e.g., on quantum Monte Carlo, Exact Diagonalization, etc. yield the solution. For more details we refer to (Georges et al 1996) for a review. Note that local-interaction diagrams are included to all orders in this non-perturbative theory. The vital energy dependence of the Weiss field ensures the qualitatively correct description of low-energy QP features as well as high-energy incoherent (Hubbard) excitations. Extensions to overcome the restriction to a k -independent self-energy, e.g. via cluster schemes, are available. But those will not be further pursued in the present text.

3.3 Combining DFT and DMFT

The first explicit promotions of DMFT to the realistic level through a merging with Kohn-Sham DFT has been realized end of the 1990s (Anisimov et al 1997; Lichtenstein and Katsnelson 1998). Importantly, since the many-body part incorporates a Hubbard-model(-like) picturing of a suitably chosen *correlated subspace*, a (partly) local-orbital representation is an essential building block of the DFT+DMFT framework. Linear-muffin-tin-orbitals (Andersen 1975), Wannier(like) functions, e.g. of maximally-localized kind (Marzari et al 2012), or projected-local orbitals (Amador et al 2008; Anisimov et al 2005) are usually in charge of that representation. The correlated subspace is understood as a quantum-numbered real-space region where

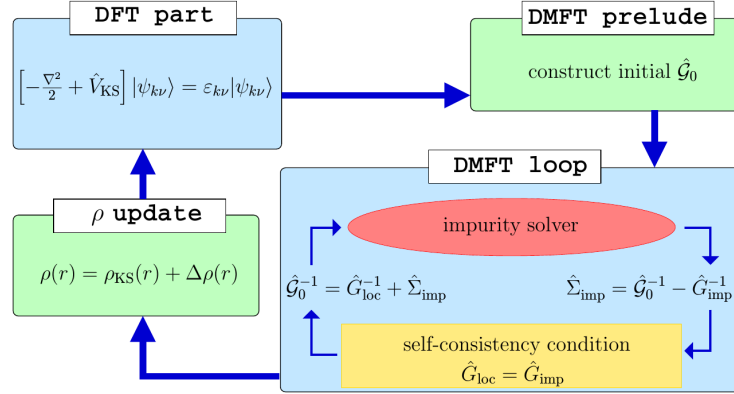


Fig. 4 State-of-the-art charge self-consistent DFT+DMFT loop (after (Lechermann et al 2006)). The calculation usually starts from a self-consistent Kohn-Sham solution. The correlated subspace is defined and the initial Weiss field \mathcal{G}_0 constructed. Afterwards, a single (or more) DMFT step is performed. The obtained self-energies are upfolded and an updated charge density $n(\mathbf{r})$ is computed. A new charge density implies a new Kohn-Sham potential, and a single new Kohn-Sham step is performed, therefrom a new Weiss field is generated, etc..

correlated electrons hide. The key interfacing blocks of the complete DFT+DMFT self-consistency cycle (Savrasov et al 2001; Minár et al 2005; Purovskii et al 2007; Grieger et al 2012) (cf. Fig. 4) are marked by the downfolding of the full-problem Bloch space to the correlated subspace, and the upfolding of the DMFT self-energy back to the original space. The main respective formulas for sites \mathbf{R} , local orbitals mm' and band indices $\nu\nu'$, read

$$G_{mm'}^{\mathbf{R},\text{imp}}(i\omega_n) = \sum_{\mathbf{k}, (\nu\nu') \in \mathcal{W}} \bar{P}_{m\nu}^{\mathbf{R}}(\mathbf{k}) G_{\nu\nu'}^{\text{bloch}}(\mathbf{k}, i\omega_n) \bar{P}_{\nu'm'}^{\mathbf{R}*}(\mathbf{k}) \quad , \quad (5)$$

$$\Delta\Sigma_{\nu\nu'}^{\text{bloch}}(\mathbf{k}, i\omega_n) = \sum_{\mathbf{R}, mm'} \bar{P}_{m\nu}^{\mathbf{R}*}(\mathbf{k}) \Delta\Sigma_{mm'}^{\mathbf{R},\text{imp}}(i\omega_n) \bar{P}_{m'\nu'}^{\mathbf{R}}(\mathbf{k}) \quad , \quad (6)$$

with \bar{P} denoting the normalized projection between Bloch space and correlated subspace (Amadon et al 2008). The object $\Delta\Sigma_{\nu\nu'}^{\text{bloch}}$ describes the k -dependent self-energy in Bloch space after double-counting correction. As for the correlated subspace, there is a choice for the range \mathcal{W} of included Kohn-Sham bands in the downfolding. The double-counting correction takes care of the fact that some correlations are already handled on the DFT level. In the upfolding operation, the charge density will also be updated with correlation effects, i.e.

$$\rho(\mathbf{r}) = \sum_{\mathbf{k}, \nu\nu'} \langle \mathbf{r} | \Psi_{\mathbf{k}\nu} \rangle \left(f(\tilde{\epsilon}_{\mathbf{k}\nu}) \delta_{\nu\nu'} + \Delta N_{\nu\nu'}(\mathbf{k}) \right) \langle \Psi_{\mathbf{k}\nu'} | \mathbf{r} \rangle \quad , \quad (7)$$

where Ψ denotes Kohn-Sham states, f the associated Fermi function and ΔN is the DMFT self-energy correction term (Lechermann et al 2006; Amadon et al 2008).

Thus, since a pure band picture is not vital in a many-body system and *real-space* excitations also matter, additional off-diagonal terms in the band index contribute in the correlated regime. This novel charge density accordingly then defines a new Kohn-Sham effective potential. Note finally that this first-principles many-body scheme works, at heart, at finite temperature T . Electron states are therefore subject to the full thermal impact, beyond sole occupational Fermi-function modification. For more formal and detailed accounts on the DFT+DMFT scheme, we refer to (Georges 2004; Kotliar et al 2006).

In oxide heterostructures, as in various other multi-atom unit cells, the correlated subspace invokes not only a single lattice site. For symmetry-equivalent sites, the self-energy is determined for a representative site and transferred to the remaining sites via the proper symmetry relations. A different impurity problem is defined for each symmetry-inequivalent site j through (Potthoff and Nolting 1999)

$$\mathcal{G}_0^{(j)}(i\omega_n)^{-1} = G^{(j)}(i\omega_n)^{-1} + \Sigma_{\text{imp}}^{(j)}(i\omega_n) \quad , \quad (8)$$

and the coupling is realized via the DFT+DMFT self-consistency condition invoking the computation of the complete lattice Green's function.

4 Selected studies of the correlated electronic structure of oxide heterostructures

There are already various applications of the DFT+DMFT approach to the problem of oxide heterostructures, and the number is expected to further grow substantially. Therefore in a short review, the choice of examples has to be highly selective and is here mainly driven by the author's interest in this field of research. We apologize for not covering many details of other interesting studies. Furthermore, albeit DFT and/or DFT+U studies of oxide heterostructures also provide relevant insight, including a discussion of such works would go beyond the limited scope of the present text.

If not otherwise stated, the materials investigations discussed in sections 4.1, 4.2 involving the author were performed using charge-selfconsistent DFT+DMFT based on a mixed-basis pseudopotential code (Meyer et al 2012) and hybridization-expansion continuous-time quantum Monte Carlo (Werner et al 2006) in the TRIQS package (Seth et al 2016) as an impurity solver. For more technical details on the implementation the reader is referred to (Grieger et al 2012).

4.1 Mott-band insulator architectures

Joining different bulk electronic phases across the interface of a heterostructure is appealing as a plausible route to emerging physics. Thermodynamics may select novel electronic states different from the original bulk states, that cope with the intriguing phase competition.

In this respect, oxide heterostructures composed of a Mott- and a band insulator belong to early studied systems, initially via experimental work on the $\text{LaTiO}_3/\text{SrTiO}_3$ (LTO/STO) interface (Ohtomo et al 2002). While STO is an ideal cubic perovskite at ambient temperature, LTO marks a distorted perovskite with orthorhombic crystal symmetry. First model-Hamiltonian Hartree-Fock studies of an Hubbard-model application to such a interface yielded an intricate phase diagram in the number of La layers and Hubbard U (Okamoto and Millis 2004). Simplified realistic DMFT for LTO/STO by (Ishida and Liebsch 2008) emphasized the structural orthorhombic-versus-tetragonal aspect of the LTO part. Transport within a Mott-band insulator heterostructure has been studied again within a model-Hamiltonian approach by (Rüegg et al 2007).

A superlattice DFT+DMFT investigation of LTO/STO (Lechermann et al 2013) revealed the realistic competition of both insulating systems stacked along the c -axis, giving rise to a metallic interface state. The correlated subspace can be chosen to be spanned by $\text{Ti-}3d(t_{2g})$ states, i.e. consists locally of three correlated orbitals. A Hubbard $U = 5$ eV and Hund's exchange $J_H = 0.7$ eV is applied in that subspace. Orbital-dependent charge transfers lead to a strong $\text{Ti-}3d(xy)$, i.e. inplane electronic, polarization in the interface TiO_2 layer. Surely, on the STO side the Ti^{4+} oxidation state with nominal $3d^0$ occupation is quickly reached, while on the LTO side the $\text{Ti}^{3+}-3d^1$ establishes and a sizable lower Hubbard band at ~ -1.1 eV is identified in the spectral function (see also Fig. 5). In those calculations, the lattice constant was fixed to the cubic STO value, but local structural relaxations on the DFT level

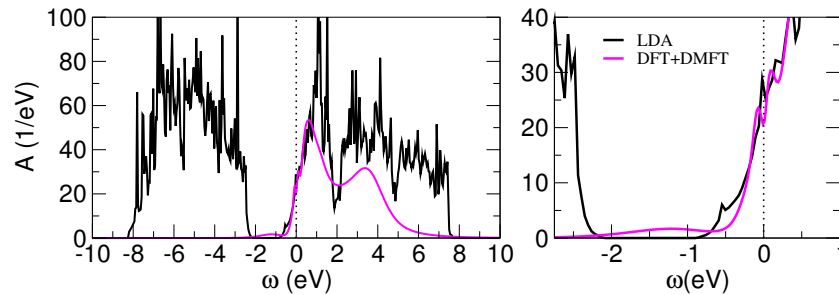


Fig. 5 Spectral information for a $\text{LaTiO}_3/\text{SrTiO}_3$ superlattice with 4 SrO and 4 LaO layers (after (Lechermann et al 2013)). Left: total spectrum, right: closer to Fermi level. Note that the DMFT correlated subspace includes only $\text{Ti}(t_{2g})$ functions, therefore the DFT+DMFT spectra is here chosen to cover also only these contributions. However of course in the charge self-consistent cycle, all states are included.

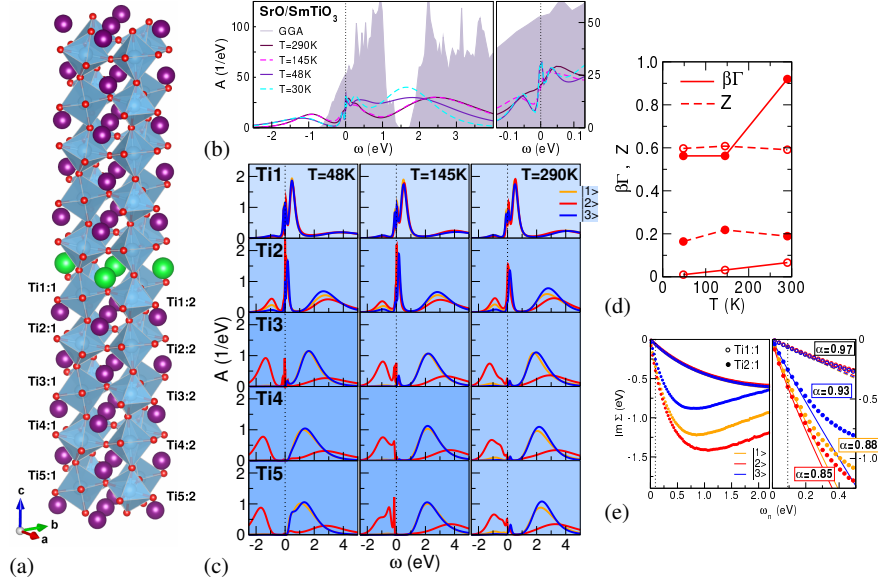


Fig. 6 Paramagnetic DFT+DMFT data of δ -doping SmTiO₃ with a SrO monolayer (after (Lechermann 2017b)). (a) 100-atom unit cell in a superlattice architecture: Sr (green), Sm (purple), Ti (blue), O (red). Two inequivalent Ti sites are handled in each TiO₂ layer. Structural relaxations are performed on the DFT(GGA) level. (b) Total spectral function at different temperatures. (c) Layer-, orbital- and T -resolved spectral function. The correlated subspace consists of three effective t_{2g} orbitals at each Ti site. (d) QP weight Z and dimensionless electron-electron scattering rate $\beta\Gamma = -Z\text{Im}\Sigma(i0^+)$ for the dominant state $|2\rangle$ in the first (open circles) and second (filled circles) TiO₂ layer. (e) Orbital-resolved imaginary part of the self-energy on the Matsubara axis. Left: larger frequency range, right: low-frequency region with fitting functions $\text{Im}\Sigma(\omega_n) = C_0 + A\omega_n^\alpha$ (dashed/full lines). Exponential-fitting cutoff n_c is denoted by the dotted line. Values $\alpha = 1$ and $C_0 = 0$ mark the Fermi-liquid regime.

were allowed. It is to be noted that the lattice degrees of freedom are an important aspect in oxide heterostructures. Simplified DFT+DMFT bulk-like studies revealed e.g. the impact of strain on the Mott-insulating state of LaTiO₃ (Dymkowski and Ederer 2014) and LaVO₃ (Sclauzero and Ederer 2015).

Even more intriguing physics may be found when starting from a doped-Mott state within the heterostructure setting. Motivated by experimental work (Moetakef et al 2012; Jackson et al 2014; Mikheev et al 2015), a first-principles many-body investigation of δ -doping the rare-earth titanates LaTiO₃, GdTiO₃ and SmTiO₃ with a single SrO layer was undertaken (Lechermann and Obermeyer 2015; Lechermann 2017b). Especially the δ -doped SmTiO₃ case displays puzzling physics in experiment, namely NFL transport that switches to FL-like characteristics upon adding further SrO layers. In the rare-earth titanate $3d(t_{2g}^1)$ series of distorted-perovskite Mott insulators, the magnetic low-temperature state changes from antiferromagnetic (AFM) to ferromagnetic (FM) with the size of the rare-earth ion. The samarium titanate is still AFM, but just on the border towards ferromagnetism. Structurally

well-defined hole doping introduced by the SrO monolayer renders SmTiO_3 metallic. The DFT+DMFT results (see Fig. 6) reveal significant spectral-weight transfer to higher energies compared to DFT, and in addition a complex layer-resolved electronic structure. While far from the doping layer the system resides in an orbital-polarized Mott-insulating state, it is conducting in an orbital-balanced manner just at the interface TiO_2 layer (cf. Fig. 6c). Both regimes are joined by an orbital-polarized doped-Mott layer with a largely renormalized QP peak at the Fermi level. Detailed analysis of the layer- and orbital-dependent self-energies shown in Fig. 6d,e indeed reveal signatures of a NFL exponent for the dominant effective t_{2g} orbital in the second, i.e. orbital-polarized doped-Mott, TiO_2 layer. Further investigations hint towards competing AFM-FM fluctuations in the Mott-critical zone as a possible cause for NFL behavior (Lechermann 2017b). A pseudogap(-like) structure in the theoretical spectral function subject to such fluctuations has indeed been identified in experimental studies (Marshall et al 2016). In an extension of this study, it was shown that the addition of further SrO layers establishes an extra band-insulating regime in the formed SrTiO_3 -like region, with a stronger inplane xy -polarized metallic layer at the boundary (Lechermann 2017a).

4.2 *Band-band insulator architectures*

The formation of a metallic twodimensional electron system (2DES) at the n -type interface between the band insulators LaAlO_3 (LAO) and SrTiO_3 (Ohtomo and Hwang 2004) has so far been the most appreciated finding in the oxide-heterostructure context. Follow-up experimental studies furthermore revealed the 2DES delicacy, e.g. the possibility for superconductivity (Reyren et al 2007) as well as magnetic order (Brinkman et al 2007) in the LAO/STO interface. A polar-catastrophe mechanism (Nakagawa et al 2006) is believed to be dominantly at the root of the 2DES build up.

In view of electronic correlations, this and related interface systems (Chen et al 2013) appear more subtle since the band-insulating constituents do not already host electrons in partially-filled d - or f - states. Nonetheless, the confirmed stabilization of magnetic and superconducting order proofs the existence of collective electronic behavior. Then, nonlocal effects might be more crucial than in the former Mott-band heterostructures. However, still relevant local correlations are evident from the coappearance of oxygen vacancies and ferromagnetism in LAO/STO (Salluzzo et al 2013). Point defects are an important ingredient of the present interface physics, and oxygen vacancies (OVs) so far appear to have major impact (Pavlenko et al 2012). In a DFT+DMFT study of the LAO/STO interface (Lechermann et al 2014) it is shown that stable ferromagnetic order needs both, OVs *and* electronic correlations. While $\text{Ti-}3d(t_{2g})$ orbitals dominate the states directly above the STO gap, an oxygen vacancy leads to an in-gap state of $\text{Ti-}3d(e_g)$ kind, here termed \tilde{e}_g . In a minimal model, the correlated electronic structure at the interface may be described by the interplay between \tilde{e}_g and an inplane xy orbital from the t_{2g} threefold (see Fig. 7). Therefore

a reduced Hubbard $U = 2.5$ eV and Hund's exchange $J_H = 0.5$ eV is appropriate in the smaller correlated subspace. Note that a dense-defect scenario is assumed in that superlattice assessment, i.e. there is an OV at every other O site in the interface TiO_2 plane. Still an in-gap \tilde{e}_g -like state at $\epsilon_{\text{IG}} \sim -1.2$ eV is well reproduced in agreement with experiment (Berner et al 2013). Close to an oxygen vacancy, the formal oxidation state of titanium is close to Ti^{3+} , i.e. again locally a $3d^1$ occupation is realized with defects. But the emergent spin polarization in the given defect limit is not of purely local kind, it develops substantial dispersive behavior (cf. Fig. 7d,e). In general, such studies show that strong electron correlations, describable within DMFT, may be introduced also in band-band insulator architectures of oxide heterostructures.

Approaching significantly lower OV concentrations in a first-principles manner asks for the handling of much larger supercells. Due to the numerical heaviness

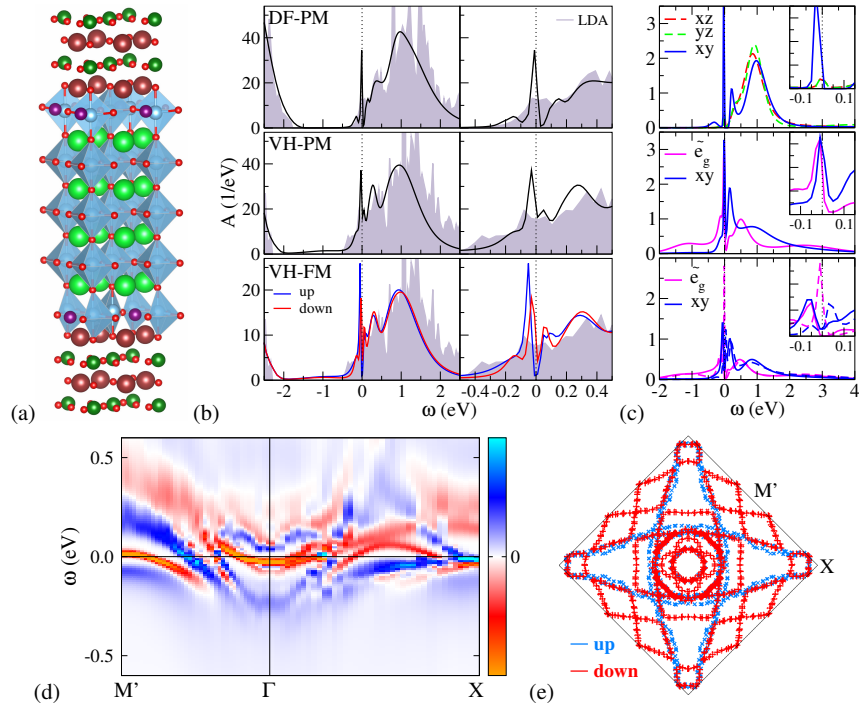


Fig. 7 Influence of oxygen vacancies in the LAO/STO interface based on DFT+DMFT calculations for a dense-defect scenario (after (Lechermann et al 2014)). (a) 80-atom superlattice, La (brown), Al (darkgreen), Sr (green), Ti (blue), O (red), OV (violet). (b) Total spectral function, left: larger window, right: smaller window. Top: defect-free paramagnetic (DF-PM), middle: vacancy-hosting paramagnetic (VH-PM) and bottom: vacancy-hosting ferromagnetic (VH-FM). (c) Local spectral function for selected effective Ti(3d) states (see text), vertical ordering as in (b). (d) spin contrast of the k -dependent spectral function $A(\mathbf{k}, \omega)$ in the ferromagnetic phase. (e) ferromagnetic Fermi surface.

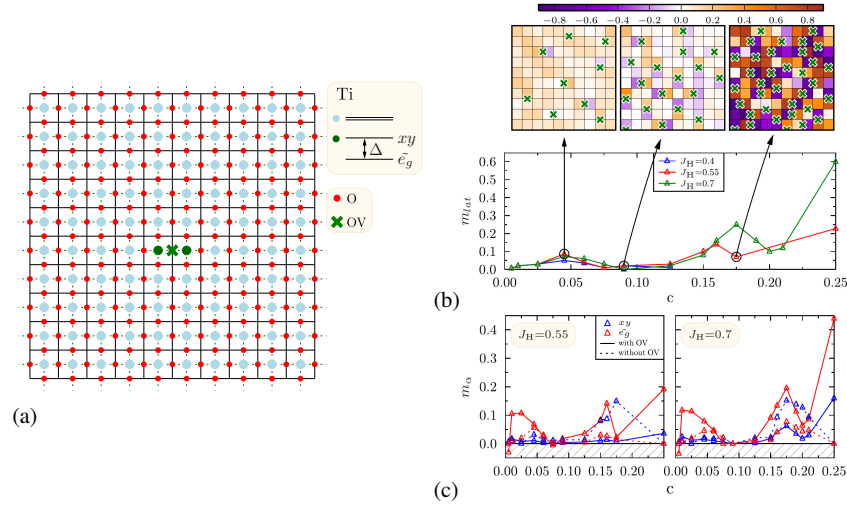


Fig. 8 Influence of oxygen vacancies in the LAO/STO interface. (after (Behrmann and Lechermann 2015)). (a) Model setting: 10×10 square lattice, two orbital per site, oxygen degrees of freedom are integrated out, nearest-neighbor hopping $t = 0.2$ eV. A crystal-field splitting $\Delta = 0.3$ eV between \bar{e}_g and xy is applied, if an OV is located nearby. (b) Top: color-coded ordered local magnetic moments on the lattice for selected OV concentration. Bottom: lattice net moment per site for different Hund's exchange J_H . (c) Orbital-resolved magnetic moment, averaged per site.

of DFT+DMFT, this is yet not easily possible. Instead, a model-Hamiltonian approach, equipped with the relevant ingredients from the dense-defect limit, appears more adequate. Figure 8 displays the setting and some main results of such an ansatz (Behrmann and Lechermann 2015). A two-orbital \bar{e}_g - xy Hubbard model is solved on a 10×10 square lattice resembling the TiO_2 interface plane. The efficient rotational-invariant slave boson (RISB) scheme (Lechermann et al 2007; Li et al 1989), employing a self-energy which has a linear-in-frequency term and a static term, is put into practise for a simplified treatment. Focussing on the magnetic order, it is shown that there are three regimes with growing number of OVs. At very small concentration, a Ruderman-Kittel-Kasuya-Yoshida (RKKY) coupling leads to FM order, whereas at larger concentration a double-exchange mechanism dominates a different FM phase. Inbetween local AFM pairs (or, in an advanced self-energy modelling, possibly singlets) result in a nearly absent net magnetic moment. This intricate OV-dependent magnetic exchange is in line with experimental findings of strongly probe-dependent magnetic response.

In parallel to the STO-based heterostructure investigations, studying the SrTiO_3 surface attracted significant attention. Interface and surface properties of a chosen oxide are often related and the comparison between both plane defects enables a better understanding of emergent phenomena. A 2DES was initially also found on the oxygen-deficient (001) surface (Santander-Syro et al 2011; Meevasana et al

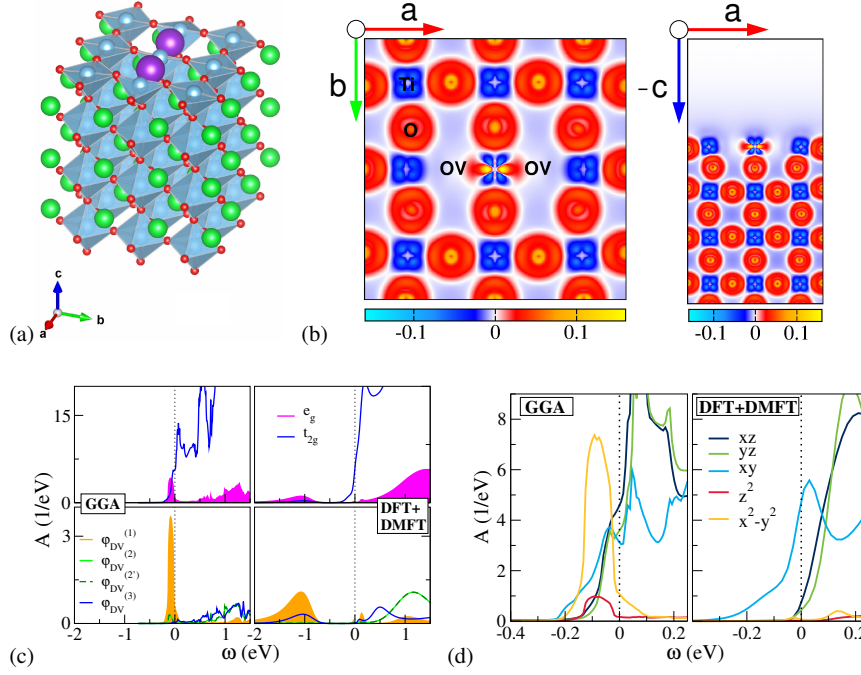


Fig. 9 Influence of a double vacancy in the SrTiO₃ (001) surface. (after (Lechermann et al 2016)). (a) 180-atom supercell with a TiO₂-terminated surface layer of STO: Sr (green), Ti (blue), O (red), OV (violet). (b) Bond charge density $n_{\text{total}}(\mathbf{r}) - n_{\text{atomic}}(\mathbf{r})$: top view (left), side view (right). (c) Spectral-weight comparison of the summed Ti(t_{2g}, e_g) (top) and of the dominant Ti-based effective orbital between DFT(GGA) (left) and DFT+DMFT (right). The $\phi_{\text{DV}}^{(1)}$ Wannier-like orbital is an effective inplane e_g orbital located on the Ti site between the OVs. (d) Low-energy spectral-weight comparison of the Ti(3d) states.

2011) and soon after also confirmed for other cleavage planes, e.g. in (111) direction (McKeown Walker et al 2014). As a difference to the LAO/STO interface, the defect-free STO surface is believed to be insulating. Due to a missing interface-driven polar-catastrophe mechanism, defects such as OVs are essential to metallize the surface. Similar to the interface spectrum, an in-gap state at a very similar position, i.e. ~ -1.3 eV, has been detected on the STO surface early on (Tanaka et al 1993). Recent DFT+DMFT considerations of the STO(001) surface with OVs indeed verified this in-gap state (Lechermann et al 2016), which is again dominantly formed by Ti-3d(e_g) weight. (cf. Fig 9). Furthermore, the low-energy structure dominated by Ti-3d(t_{2g}) states is also in accordance with experiment. A double-vacancy defect provided the best matching with experiment, however only two distinct vacancy configuration were examined because of the large numerical effort. Nonetheless, the spectral separation of e_g at high energy and t_{2g} is a clear generic feature of the study. Conventional DFT is not sufficient to provide this orbital separation (cf. Fig. 9c,d).

4.3 Further investigations

So far, the present review mainly focussed on early-transition-metal titanate heterostructures, but theoretical work also dealt with other oxide designs. For instance, the late-transition-metal rare-earth (*R*) nickelate series $RNiO_3$ provides important material building blocks, too (Hwang et al 2013). Originally, there was the idea to realize cuprate-like physics within nickelates by proper heterostructuring (Hansmann et al 2009; Han et al 2011), however experimental success remains absent. Bulk perovskite-like vanadates split into correlated metals, e.g. $SrVO_3$ and $CaVO_3$, and Mott insulators, e.g. $LaVO_3$ and YVO_3 . Heterostructures based on $SrVO_3$ were studied in view of a possible loss of metallicity in a small-layer limit (Okamoto 2011; Zhong et al 2015). Moreover, transition-metal oxides from the $4d$ and $5d$ series serve as further building blocks. For instance, the $4d^4$ physics of strontium and/or calcium ruthenates poses a longstanding problem, which can be tuned by heterostructuring (Si et al 2017).

5 Outlook

The research field of oxide heterostructures will remain promising, on a basic-research level well as in view of possible technical applications. Until now, only a few materials classes have been utilized and there are vast ways of combinations, both in different materials as in different geometries. In addition, the opening towards more general hybrid heterostructures, e.g. with Dirac materials, has just started and will lead to novel phenomena. Detailed studies of challenging spin-, charge- or pairing instabilities of oxide heterostructures are still at its infancy and expectations are high for new surprising findings. Furthermore, the recent focus on the nonequilibrium regime in strongly correlated matter will find an ideal playground in this class of designed materials.

The DFT+DMFT method, and future extensions to it, has the chance to pave the roads towards a new era in materials science, highlighting the many-body character in key functionalities. A better understanding and general appreciation of the intriguing interplay between electron correlation and materials chemistry is believed to be at the heart of this endeavor.

Acknowledgements Support by the DFG LE-2446/4-1 project “Design of strongly correlated materials” is acknowledged.

References

Amadon B, Lechermann F, Georges A, Jollet F, Wehling TO, Lichtenstein AI (2008) Plane-wave based electronic structure calculations for correlated materials using dynamical mean-field the-

- ory and projected local orbitals. *Phys Rev B* 77:205,112
- Andersen OK (1975) Linear methods in band theory. *Phys Rev B* 12:3060
- Anisimov VI, Poteryaev AI, Korotin MA, Anokhin AO, Kotliar G (1997) First-principles calculations of the electronic structure and spectra of strongly correlated systems: dynamical mean-field theory. *J Phys: Condens Matter* 9:7359
- Anisimov VI, Kondakov DE, Kozhevnikov AV, Nekrasov IA, Pchelkina ZV, Allen JW, Mo SK, Kim HD, Metcalf P, Suga S, Sekiyama A, Keller G, Leonov I, Ren X, Vollhardt D (2005) Full orbital calculation scheme for materials with strongly correlated electrons. *Phys Rev B* 71:125,119
- Bednorz JG, Müller KA (1986) Possible hightc superconductivity in the Ba-La-Cu-O system. *Z Physik B - Condensed Matter* 64:189
- Behrmann M, Lechermann F (2015) Interface exchange processes in LaAlO₃/SrTiO₃ induced by oxygen vacancies. *Phys Rev B* 92:125,148
- Berner G, Sing M, Fujiwara H, Yasui A, Saitoh Y, Yamasaki A, Nishitani Y, Sekiyama A, Pavlenko N, Kopp T, Richter C, Mannhart J, Suga S, , Claessen R (2013) Direct k-Space mapping of the electronic structure in an oxide-oxide interface. *Phys Rev Lett* 110:247,601
- Brinkman A, Huijben M, van Zalk M, Huijben J, Zeitler U, Maan JC, van der Wiel WG, Rijnders G, Blank DHA, Hilgenkamp H (2007) Magnetic effects at the interface between non-magnetic oxides. *Nature Mater* 6:493
- Chakhalian J, Freeland JW, Millis AJ, Panagopoulos C, Rondinelli JM (2014) Emergent properties in plane view: Strong correlations at oxide interfaces. *Rev Mod Phys* 86:1189
- Chen YZ, Bovet N, Trier F, Christensen DV, Qu FM, Andersen NH, Kasama T, Zhang W, Giraud R, Dufouleur J, Jespersen TS, Sun JR, Smith A, Nygård J, Lu L, Büchner B, Shen BG, Linderoth S, Pryds N (2013) A high-mobility two-dimensional electron gas at the spinel/perovskite interface of γ -Al₂O₃/SrTiO₃. *Nat Commun* 4:1372
- Dymkowski K, Ederer C (2014) Strain-induced insulator-to-metal transition in LaTiO₃ within DFT+DMFT. *Phys Rev B* 89:161,109(R)
- Eckstein JN, Bozovic I (1995) High-temperature superconducting multilayers and heterostructures grown by atomic layer-by-layer molecular beam epitaxy. *Annu Rev Mater Sci* 25:679
- Georges A (2004) in Lectures on the Physics of Highly Correlated Electron Systems VIII, AIP Conference Proceedings 715, chap 3
- Georges A, Kotliar G (1992) Hubbard model in infinite dimensions. *Phys Rev B* 45:6479
- Georges A, Kotliar G, Krauth W, Rozenberg MJ (1996) Dynamical mean-field theory of strongly correlated fermion systems and the limit of infinite dimensions. *Rev Mod Phys* 68:13
- Grieger D, Piefke C, Peil OE, Lechermann F (2012) Approaching finite-temperature phase diagrams of strongly correlated materials: A case study for V₂O₃. *Phys Rev B* 86:155,121
- Han MJ, Wang X, Marianetti CA, Millis AJ (2011) Dynamical mean-field theory of nickelate superlattices. *Phys Rev Lett* 107:206,804
- Hansmann P, Yang X, Toschi A, Khaliullin G, Andersen OK, Held K (2009) Turning a nickelate fermi surface into a cupratelike one through heterostructuring. *Phys Rev Lett* 103:016,401
- Hwang HY, Iwasa Y, Kawasaki M, Keimer B, Nagaosa N, Tokura Y (2012) Emergent phenomena at oxide interfaces. *Nature Materials* 11:103
- Hwang J, Son J, Zhang JY, Janotti A, Van de Walle CG, Stemmer S (2013) Structural origins of the properties of rare earth nickelate superlattices. *Phys Rev B* 87:060,101(R)
- Imada M, Fujimori A, Tokura Y (1998) Metal-insulator transitions. *Rev Mod Phys* 70:1039
- Ishida H, Liebsch A (2008) Origin of metallicity of LaTiO₃/SrTiO₃ heterostructures. *Phys Rev B* 77:115,350
- Jackson CA, Zhang JY, Freeze CR, Stemmer S (2014) Quantum critical behaviour in confined SrTiO₃ quantum wells embedded in antiferromagnetic SmTiO₃. *Nat Commun* 5:4258
- Keimer B, Moore JE (2017) The physics of quantum materials. *Nat Phys* 13:1045
- Kotliar G, Savrasov SY, Haule K, Oudovenko VS, Parcollet O, Marianetti CA (2006) Electronic structure calculations with dynamical mean-field theory. *Rev Mod Phys* 78:865
- Lechermann F (2017a) First-principles many-body investigation of correlated oxide heterostructures: Few-layer-doped SmTiO₃. arXiv:170908875

- Lechermann F (2017b) Unconventional electron states in δ -doped SmTiO_3 . *Sci Rep* 7:1565
- Lechermann F, Obermeyer M (2015) Towards mott design by δ -doping of strongly correlated titanates. *New J Phys* 17:043,026
- Lechermann F, Georges A, Poteryaev A, Biermann S, Posternak M, Yamasaki A, Andersen OK (2006) Dynamical mean-field theory using wannier functions: a flexible route to electronic structure calculations of strongly correlated materials. *Phys Rev B* 74:125,120
- Lechermann F, Georges A, Kotliar G, Parcollet O (2007) Rotationally invariant slave-boson formalism and momentum dependence of the quasiparticle weight. *Phys Rev B* 76:155,102
- Lechermann F, Boehnke L, Grieger D (2013) Formation of orbital-selective electron states in $\text{LaTiO}_3/\text{SrTiO}_3$ superlattices. *Phys Rev B* 87:241,101(R)
- Lechermann F, Boehnke L, Grieger D, Piefke C (2014) Electron correlation and magnetism at the $\text{LaAlO}_3/\text{SrTiO}_3$ interface: A DFT+DMFT investigation. *Phys Rev B* 90:085,125
- Lechermann F, Jeschke HO, Kim AJ, Backes S, Valentí R (2016) Electron dichotomy on the SrTiO_3 defect surface augmented by many-body effects. *Phys Rev B* 93:121,103(R)
- Li T, Wölfle P, Hirschfeld PJ (1989) Spin-rotation-invariant slave-boson approach to the Hubbard model. *Phys Rev B* 40:6817
- Lichtenstein AI, Katsnelson M (1998) Ab initio calculations of quasiparticle band structure in correlated systems: LDA++ approach. *Phys Rev B* 57:6884
- Marshall PB, Mikheev E, Raghavan S, Stemmer S (2016) Pseudogaps and emergence of coherence in two-dimensional electron liquids in SrTiO_3 . *Phys Rev Lett* 117:046,402
- Marzari N, Mostofi AA, Yates JR, Souza I, Vanderbilt D (2012) Maximally localized Wannier functions: Theory and applications. *Rev Mod Phys* 84:1419
- McKeown Walker S, de la Torre A, Bruno FY, Tamai A, Kim TK, Hoesch M, Shi M, Bahramy MS, King PC, Baumberger F (2014) Control of a two-dimensional electron gas on $\text{SrTiO}_3(111)$ by atomic oxygen. *Phys Rev Lett* 113:177,601
- Meevasana W, King PDC, He RH, Mo SK, Hashimoto M, Tamai A, Songsiririthigul P, Baumberger F, Shen ZX (2011) Creation and control of a two-dimensional electron liquid at the bare SrTiO_3 surface. *Nat Mat* 10:114
- Metzner W, Vollhardt D (1989) Correlated lattice fermions in $d = \infty$ dimensions. *Phys Rev Lett* 62:324
- Meyer B, Elsässer C, Lechermann F, Fähnle M (2012) FORTRAN 90 program for mixed-basis-pseudopotential calculations for crystals
- Mikheev E, Freeze CR, Isaac BJ, Cain TA, Stemmer S (2015) Separation of transport lifetimes in SrTiO_3 -based two-dimensional electron liquids. *Phys Rev B* 91:165,125
- Minár J, Chioncel L, Perlov A, Ebert H, Katsnelson MI, Lichtenstein AI (2005) Multiple-scattering formalism for correlated systems: A kkr-dmft approach. *Phys Rev B* 72:045,125
- Moetakef P, Jackson CA, Hwang J, Balents L, Allen SJ, Stemmer S (2012) Toward an artificial mott insulator: Correlations in confined high-density electron liquids in SrTiO_3 . *Phys Rev B* 86:201,102(R)
- Mott NF, Peierls R (1937) Discussion of the paper by de Boer and Verwey. *Proc Phys Soc* 49:72
- Nakagawa N, Hwang HY, Muller DA (2006) Why some interfaces cannot be sharp. *Nature Mater* 5:204
- Ohtomo A, Hwang HY (2004) A high-mobility electron gas at the $\text{LaAlO}_3/\text{SrTiO}_3$ heterointerface. *Nature* 427:423
- Ohtomo A, Muller DA, Grazul JL, Hwang HY (2002) Artificial charge-modulation in atomic-scale perovskite titanate superlattices. *Nature* 419:378
- Okamoto S (2011) Anomalous mass enhancement in strongly correlated quantum wells. *Phys Rev B* 84:201,305(R)
- Okamoto S, Millis AJ (2004) Electronic reconstruction at an interface between a Mott insulator and a band insulator. *Nature* 428:630
- Pavlenko N, Kopp T, Tsymbal EY, Mannhart J, Sawatzky GA (2012) Oxygen vacancies at titanate interfaces: Two-dimensional magnetism and orbital reconstruction. *Phys Rev B* 86:064,431
- Potthoff M, Nolting W (1999) Surface metal-insulator transition in the Hubbard model. *Phys Rev B* 59:2549

- Pourovskii LV, Amadon B, Biermann S, Georges A (2007) Self-consistency over the charge density in dynamical mean-field theory: A linear muffin-tin implementation and some physical implications. *Phys Rev B* 76:235,101
- Reyren N, Thiel S, Caviglia AD, Kourkoutis LF, Hammerl G, Richter C, Schneider CW, Kopp T, Rüetschi AS, Jaccard D, Gabay M, Müller DA, Triscone JM, Mannhart J (2007) Superconducting interfaces between insulating oxides. *Science* 317:1196
- Rüegg A, Pilgram S, Sigrist M (2007) Aspects of metallic low-temperature transport in Mott-insulator/band-insulator superlattices: Optical conductivity and thermoelectricity. *Phys Rev B* 75:195,117
- Salluzzo M, Gariglio S, Stornaiuolo D, Sessi V, Rusponi S, Piamonteze C, DeLuca GM, Minola M, Marré D, Gadaleta A, Brune H, Nolting F, Brookes NB, Ghiringhelli G (2013) Origin of interface magnetism in $\text{BiMnO}_3/\text{SrTiO}_3$ and $\text{LaAlO}_3/\text{SrTiO}_3$ heterostructures. *Phys Rev Lett* 111:087,204
- Santander-Syro AF, Copie O, Kondo T, Fortuna F, Pailhè S, Weht R, Qiu XG, Bertran F, Nicolaou A, Taleb-Ibrahimi A, Fèvre PL, Herranz G, Bibes M, Reyren N, Apertet Y, Lecoœur P, Barthélémy A, Rozenberg MJ (2011) Two-dimensional electron gas with universal subbands at the surface of SrTiO_3 . *Nature* 469:189
- Savrasov SY, Kotliar G, Abrahams E (2001) Correlated electrons in δ -plutonium within a dynamical mean-field picture. *Nature* 410:793
- Sclauzero G, Ederer C (2015) Structural and electronic properties of epitaxially strained LaVO_3 from density functional theory and dynamical mean-field theory. *Phys Rev B* 92:235,112
- Seth P, Krivenko I, Ferrero M, Parcollet O (2016) TRIQS/CTHYB: A continuous-time quantum monte carlo hybridisation expansion solver for quantum impurity problems. *Comput Phys Commun* 200:274
- Si L, Janson O, Li G, Zhong Z, Liao Z, Koster G, Held K (2017) Quantum anomalous hall state in ferromagnetic SrRuO_3 (111) bilayers. *Phys Rev Lett* 119:026,402
- Stemmer S, Millis AJ (2013) Quantum confinement in oxide quantum wells. *MRS Bulletin* 38:1032
- Tanaka H, Matsumoto T, Kawai T, Kawai S (1993) Surface structure and electronic property of reduced $\text{SrTiO}_3(100)$ surface observed by scanning tunneling microscopy/spectroscopy. *Jpn J Appl Phys* 32:1405
- Werner P, Comanac A, de' Medici L, Troyer M, Millis AJ (2006) Continuous-time solver for quantum impurity models. *Phys Rev Lett* 97:076,405
- Zhong Z, Wallerberger M, Tomczak JM, Taranto C, Parragh N, Toschi A, Sangiovanni G, Held K (2015) Electronics with correlated oxides: $\text{SrVO}_3/\text{SrTiO}_3$ as a mott transistor. *Phys Rev Lett* 114:246,401
- Zubko P, Gariglio S, Gabay M, Ghosez P, Triscone JM (2011) Interface physics in complex oxide heterostructures. *Annu Rev Condens Matter Phys* 2:141